Correlation between structural features and mechanical properties of boron nitride fibres derived from alkylaminoborazines

Philippe Miele[a,*], Bérangère Toury[a], Fernand Chassagneux[a], René Fulchiron[b]

[a] *Laboratoire des Multimatériaux et Interfaces, UMR CNRS 5615, Université Claude Bernard-Lyon 1, 43 Bd du 11 Novembre 1918, 69622 Villeurbanne Cedex, France*
[b] *Laboratoire des Matériaux Polymères et des Biomatériaux, UMR CNRS 5627, Université Claude Bernard-Lyon 1, 43 Bd du 11 Novembre 1918, 69622 Villeurbanne Cedex, France*

Abstract

The microstructure and texture of a series of four boron nitride fibres prepared from three alkylaminoborazines 2,4,6-[(CH$_3$)$_2$N]$_3$B$_3$N$_3$H$_3$ (**1**), 2,4-[(CH$_3$)$_2$N]$_2$-6-(CH$_3$HN)B$_3$N$_3$H$_3$ (**2**) and 2-[(CH$_3$)$_2$N]-4,6-(CH$_3$HN)$_2$B$_3$N$_3$H$_3$ (**3**) have been studied by means of transmission electronic microscopy (TEM) and polarized light microscopy (PLM) on the basis of relevant X-ray diffraction (XRD) and Raman spectroscopy data. TEM results indicate that the general structure of the fibres consists in three concentric parts with a gradual increase in the crystallites size from the outer region to the core of the fibres. The grains appear to be randomly distributed in the fibre prepared from **1** whereas a pronounced orientation of crystallites is found in the fibres derived from **2** and **3**. This local feature was extended to a larger scale by the use of PLM, which showed that the orientation of crystallites with respect to the fibre axis is improved within the fibres prepared, respectively, from **1**, **2** and **3**. The comparison of these results evidenced a correlation between microstructural and textural properties and the mechanical performances of the studied boron nitride fibres. Thus, this work exemplified that mechanical properties of BN fibres are closely associated with both a good crystallization state, e.g. large crystallites and a preferred mean alignment of BN crystallites following their (0 0 2) planes (i.e. planes of hexagons) in a direction parallel to the fibre axis.
© 2004 Elsevier Ltd. All rights reserved.

Keywords: Boron nitride fibres; Alkylaminoborazines; Crystallinity; TEM; PLM

1. Introduction

The graphite-like modification of boron nitride, the hexagonal polymorph h-BN, displays a wide range of unique properties especially a high chemical and thermal stability and oxidation resistance largely superior to that of graphite.[1] Thus, BN based composites are of particular interest for applications at high temperature even though the use of this ceramic could be extended regarding its insulating properties. The development of such composites is restricted by the fact that BN fibres are not commercially available which has motivated several studies devoted to their elaboration particularly in our group [2–4] (and ref. therein).

Recently, we reported progresses in the achievement on high performances boron nitride fibres prepared from aminoborazines-based polymers. Three borazinic precursors 2,4,6-[(CH$_3$)$_2$N]$_3$B$_3$N$_3$H$_3$ (**1**), 2,4-[(CH$_3$)$_2$N]$_2$-6-(CH$_3$HN)B$_3$N$_3$H$_3$ (**2**) and 2-[(CH$_3$)$_2$N]-4,6-(CH$_3$HN)$_2$B$_3$N$_3$H$_3$ (**3**) as well as derived polyborazines have been studied within the goal of evidence relationships between the mechanical properties of the final ceramic fibres and the nature of the starting molecular precursors as well as the derived polymers.[3,4] Thus, the thermolysis of **1** and **2** led to polyborazines **4** and **5**, respectively, whereas two different polymers **6** and **7** have been obtained from **3**. The main conclusion of these works is that the melt-spinnability of the as-prepared polyalkylaminoborazines is mostly improved by the presence of bridged inter-ring −N(CH$_3$)− groups to the detriment of direct B−N intercyclic bonds. Actually, the spinning properties increase in the order **4** < **5** < **6** < **7** which could be

* Corresponding author. He is also with the Institut Universitaire de France (IUF).
  E-mail address: miele@univ-lyon1.fr (P. Miele).

related to the increased proportion of bridging groups quoted above between the B_3N_3 rings within this series. Moreover, it must be noticed that **6** and **7** come from the same monomer which underline in addition the importance of the control of the polycondensation reaction to improve the spinning capabilities of the polyborazines. In much in the same way, we also showed that improvement in the spinnability of the polyborazines has for consequence an increase in the mechanical properties of the resulting BN fibres. In summary, these conclusions demonstrated that the melt-spinnability of the polyalkylaminoborazines and the mechanical properties of the derived ceramic fibres are closely related to the nature and the structure of the molecular and polymeric precursors. Furthermore, we mentioned in these papers that following the example of carbon fibres, the mechanical properties of BN fibres depend in a large extent on the structural state of the BN phase. For example, the X-ray diffraction analyses of BN fibres allow to show a possible preferred orientation of the (0 0 2) planes in the material in relation with their mechanical properties. In the same vein, the crystalline quality of the fibres has been studied by Raman scattering exemplifying an increase in crystallites size for fibres obtained from **4**, **5**, **6** and **7**, respectively. The examination of both XRD and Raman scattering data led us to deduce that the mechanical properties of BN fibres increase with the improvement of preferred orientation of the (0 0 2) basal planes along the fibre axis, as well as the increase of the crystalline quality, i.e. crystallites size.[2,4]

Thus, these preliminary results are completed in the present work by the study of structural and textural state of boron nitride fibres by techniques providing either different resolution capabilities and/or giving the same kind of informations at different scales. Previously described boron nitride fibres prepared from **4**, **5**, **6** and **7** have been thoroughly characterised by transmission electron microscopy (TEM) and polarized light microscopy (PLM) by taking into account useful X-ray diffraction and Raman scattering data, and the conclusions have been confronted in relation with their mechanical properties.

2. Experimental

2.1. Preparation of BN fibres

Achievement of the studied BN fibres has been fully reported in previous papers. The preparation of polyborazines **4**, **5** and **6** by thermal polycondensation of alkylaminoborazines 2,4,6-[$(CH_3)_2N]_3B_3N_3H_3$ (**1**), 2,4-[$(CH_3)_2N]_2$-6-$(CH_3HN)B_3N_3H_3$ (**2**) and 2-[$(CH_3)_2N$]-4,6-$(CH_3HN)_2B_3N_3H_3$ (**3**), respectively, and their subsequent conversion into boron nitride fibres **4.1**, **5.1** and **6.1** was described in a first paper.[3] The improvement in the preparation process of a polyborazine **7** derived from **3** allows the fabrication of BN fibres **7.1** with enhanced mechanical properties as it was reported in a second paper in.[4] Table 1 summarized the

Table 1
Significant properties of polyborazines **4**, **5**, **6** and **7** and fibres **4.1**, **5.1**, **6.1** and **7.1**

Run (fibre)	4.1	5.1	6.1	7.1
T_g (°C)	45	48	56	65
Ceramic yield (%)[a]	50.1	52.0	52.4	51.6
Spinning temperature (°C)	195	120	140	165
Diameter of BN fibre (µm)	30	14.8	10.7	10.7
Strength σ^R (GPa)	_[b]	0.51	0.69	1.37
Young's modulus E (GPa)	_[b]	67	170	210
Raman scattering/E_{2g} mode (cm^{-1})	1369.8	1368.3	1367.4	1367.0
$R_{(0\,0\,2/1\,0)}$	–	10.4	62.5	66.7

[a] Under ammonia from 25 to 600 °C and nitrogen between 600 and 1000 °C.
[b] Fibres **4.1** could not be tested due to their brittleness.

main characteristics of used polymers and ensuing ceramic fibres.

2.2. Structural characterisation

X-ray diffraction (XRD) analyses were performed on a Philips PW 3710/3020 diffractometer using a Cu Kα radiation source ($\lambda = 1.54$ Å) in the 2θ range 10–90°. Patterns with peak positions and relative intensities using the (0 0 2) peak as a reference ($I_{(0\,0\,2)} = 100\%$) were matched against reference patterns from the JCPDS database.[5] Raman diffusion spectra were recorder with a Hololab 785 (series 500) Raman spectrometer with $\lambda = 784$ nm. Transmission electronic micrographs were obtained with a Topcon EMB-002B microscope in both imaging and diffraction modes (diffraction patterns were obtained on 0.5 µm selected areas-SAED patterns) on fragments of fibres embedded in an epoxy resin then cut with an ultramicrotom (LEICAS) as fully described in ref.[6] An Optiphot-Pol (Nikon) microscope equipped with crossed polarizers and a rotating stage was used to investigate crystallites orientation in the fibres with polarized light. The orientation of (0 0 2) crystallographic planes is revealed by transmitted light for an angle of 45° between the fiber and the polarizer direction.

3. Results and discussion

The preparation of BN fibres **4.1**, **5.1**, **6.1** and **7.1** from polymers derived from alkylaminoborazines 2,4,6-[$(CH_3)_2N]_3B_3N_3H_3$ (**1**), 2,4-[$(CH_3)_2N]_2$-6-$(CH_3HN)B_3N_3H_3$ (**2**) and 2-[$(CH_3)_2N$]-4,6-$(CH_3HN)_2B_3N_3H_3$ (**3**) has been previously reported by our group.[3,4] The procedure is briefly described in the experimental part and details can be found in the above-mentioned papers.

Raman spectroscopy and X-ray diffraction have been used in order to acquire structural and textural preliminary informations on these fibres. For example, in Raman spectroscopy, the E_{2g} mode peak around 1370 cm^{-1} characteristic of h-BN, is known to broaden and shift to higher frequency when the
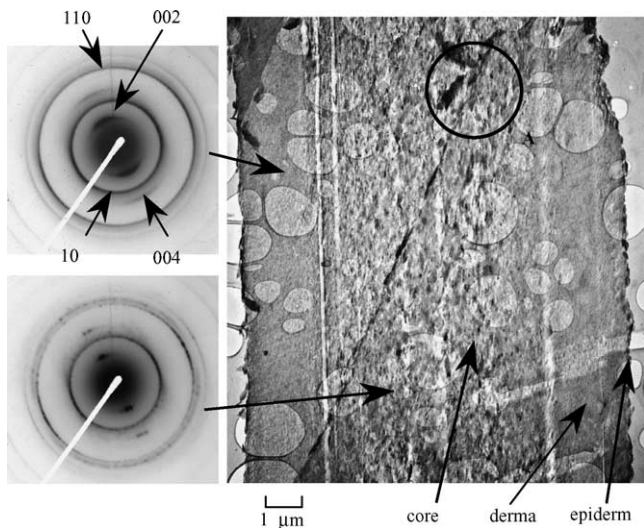
Fig. 1. TEM micrograph of a longitudinal section of BN fibre **4.1** and corresponding SAD patterns.

Fig. 2. TEM micrographs of a longitudinal section of BN fibre **5.1**.

crystallite size decreases.[7] In the examples presented therein, this peak appears in the expected region (Table 1) and is shifted to lower frequencies while sharpening following the order **4.1**, **5.1**, **6.1** and **7.1** which reflects a gradual increase in the crystallites size.

3.1. TEM studies of fibres **4.1**, **5.1**, **6.1** and **7.1**

The microstructure and texture of BN fibres **4.1**, **5.1**, **6.1** and **7.1** have been studied on longitudinal sections (knife plane parallel to the fibre axis) in order to confirm the microstructural organization revealed by X-ray diffraction and Raman scattering.

Fig. 1 shows a longitudinal section of fibre **6.1**. The bright field (BF) image evidences that the fibre is constituted of three distinct regions, with a thin outer layer of $\sim$0.2 μm namely the epiderm, a region which extends on 2 μm in thickness namely the derma, and the core of the fibre. From this image, it seems that the latter region is well-crystallized whereas the derma consists in finer nanocrystallites. This feature has been already observed for poly(methylamino)borazine-derived boron nitride fibres.[6] It is probably correlated to a lower crystallization process at the periphery in relation to a slight enrichment in nitrogen near the surface due to the exit flux of nitrogen-rich gases during the pyrolysis. However, it should be noted that this specific point is still under investigation.

In this particular case, we can also observe a very crystallized area which expands diagonally in the core of the fibre (A). This feature is probably due to a local crystallization phenomenon occurring at high temperature. Selected-area diffraction (SAD) patterns of the derma and the core (Fig. 1) display the rings corresponding to (1 1 0), (0 0 4), (1 0) and (0 0 2) planes characteristic of hexagonal boron nitride.[6] However, the resolution of diffraction rings improves start-
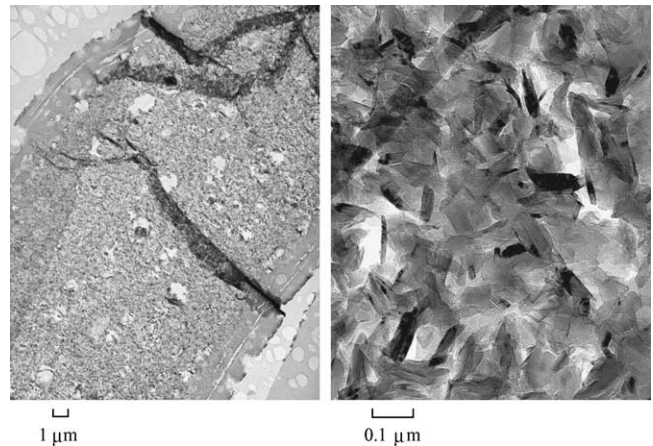
ing from the derma to the core. In particular, (0 0 2) and (1 0) diffraction rings are finer in the core compared with those of the derma demonstrating that the mean crystallite size is larger in the core. Additionally, discontinuities in electron diffraction rings also show that it exists preferential orientations, particularly (0 0 2) planes for which the diffraction is reduced to a semicircle. Remarkable is also that the (0 0 2) semicircle sharpens from the derma to the core showing a better orientation of the (0 0 2) planes, i.e. the planes of hexagons, parallel to the fibre axis.[1] However, it should be noted that one cannot refer to the direction given by the (0 0 2) semicircles of the SAD patterns because there is a shift of angle between the image mode and the diffraction mode.

Fig. 2 shows bright field (BF) TEM micrographs of the fibre **5.1**. This analysis has been relatively delicate to conduct because of the brittleness of the material and also in relation with the presence of heterogeneities in the structure (cavities, cleavage) which probably come partly from the cutting of the samples. As in the case of fibre **6.1** quoted above, the same three regions could be observed in the low magnification image. However, the core of the fibre displays a microstructure with numerous voids and cavities. At higher magnification, fine microstructural details are resolved and the micrograph shows that the crystallites are randomly oriented compared to the fibres axis in accordance with the results of X-ray analysis.[3] The same kind of conclusion could be drawn in the case of fibre **4.1**. The fibre is constituted of three regions as the two others and numerous flaws are visible especially in the core of the fibre (Fig. 3). In contrast to SAD patterns of **6.1** (Fig. 1), those of **4.1** display a large (0 0 2) ring and poorly resolved (1 0), (0 0 4) and (1 1 0) rings. Therefore, SAD analyses reflect the poor crystalline quality as well as no microstructural ordering of the sample. In addition, the large (0 0 2) nearly continuous ring is consistent with the lack of orientation of the corresponding planes. This

---

[1] Indeed, for hexagonal plans randomly oriented, the diffraction spot would constitute a circle of regular intensity whereas for a perfectly oriented crystal, the spot would be theoretically reduced to an infinitely small point.
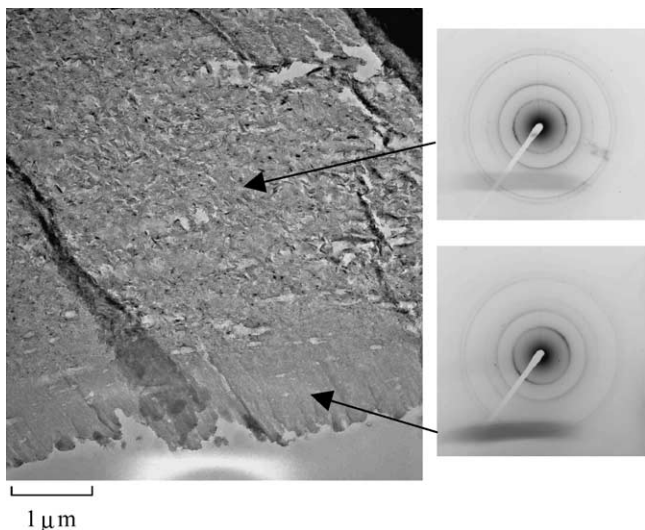
Fig. 3. TEM micrograph of a longitudinal section of BN fibre **6.1** and corresponding SAD patterns.

absence of preferred orientation in fibres **4.1** and **5.1** can be probably correlated to the low mechanical properties of both fibres.

Finally, a high-performances BN fibre **7.1** has been analysed following the same way. Fig. 4 presents a BF TEM image of this fibre and the SAD patterns of different regions of the fibre. As in the case of the fibre **6.1**, three regions can be observed but the epiderm and the derma are thinner than for fibre **6.1**. Similarly, the mean crystallite size increases from the epiderm to the core in accordance with the decrease in the broadening of the (0 0 2) and (1 0 0) rings in the SAD patterns of different regions. Since discontinuities are emphasized within the same sequence starting from epiderm, derma to the core particularly for ring associated with the (0 0 2) reflection, it can be concluded that the textural orientation is more pronounced in the core of the fibre. This orientation evidenced at the probe scale could be extended at a higher magnification by comparison between dark field and bright field images (Fig. 5) of the same part of a fibre from the core (bottom right) to the derma (top left). The images are superimposed perfectly which highlights the high level of orientation of the (0 0 2) planes in the core as well in the derma. However, as it has been mentioned above the crystallites are larger in the core.

3.2. PLM studies of fibres **4.1**, **5.1**, **6.1** and **7.1**

Another set of characterisations were carried out by using PLM. This technique has been widely used for the rapid texture investigation of carbon fibres exploiting the optical anisotropy of graphite.[8–10] It should be of great interest for BN fibres by taking into account the close relationship between the structures of these ceramics. Actually, since h-BN is an uniaxial crystal with the optical axis along the *c* axis, it presents consequently anisotropic optical properties, i.e.
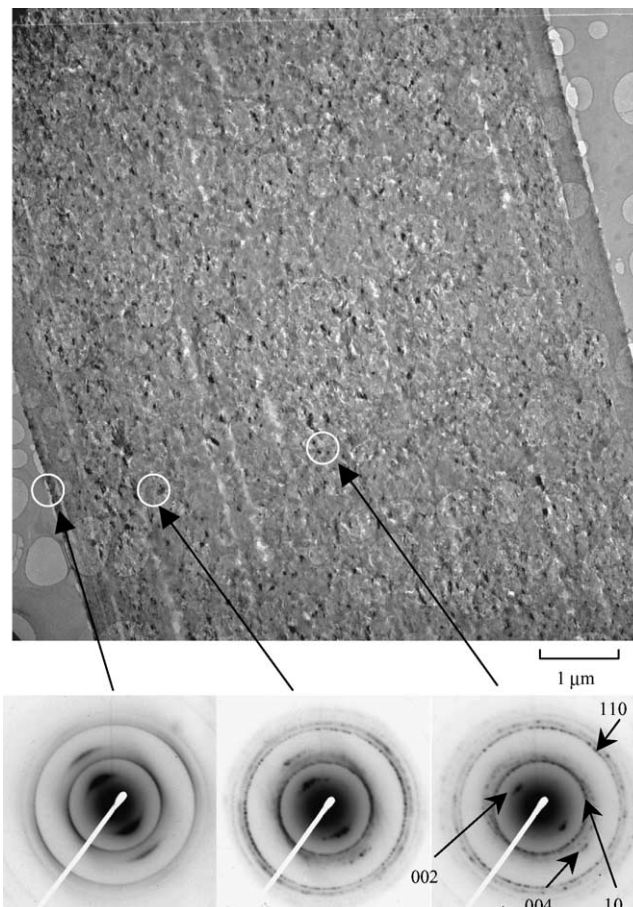

Fig. 4. TEM micrograph of a longitudinal section of BN fibre **7.1** and corresponding SAD patterns.

birefringence, as previously detailed for graphite.[11] Thus, a BN crystal observed with a parallel beam of polarized light between crossed polarizer and analyzer shows a different behaviour depending on its orientation. If the crystal is oriented such as the *c* axis is perpendicular to the beam, i.e. in the observation plane, we should observe alternatively four
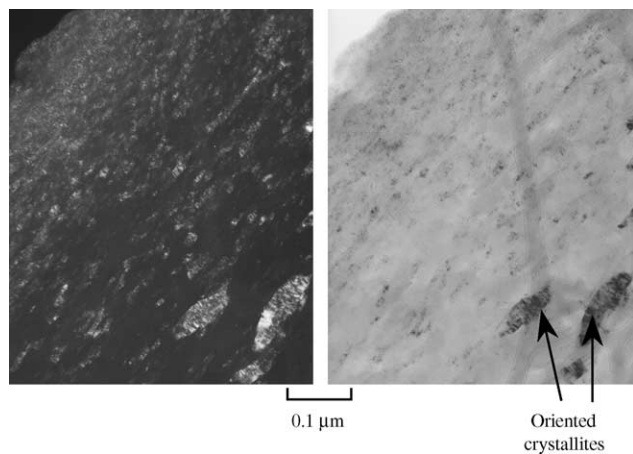

Fig. 5. Dark field (left) and bright field (right) TEM micrographs of a part of fibre **7.1**.

straightforward maxima in intensity and four complete extinctions, these extrema being separated by an angle of 45°, during the rotation of the stage. The first extinction appears when the *c* axis is parallel to the polarizer direction whereas the first maximum in intensity appears after a 45° angle rotation of the *c* axis with respect to the polarizer direction. In the case of observations of a fibre disposed such as its axis is parallel to the plane of observation, the brightness and the uniformity of the reflected light observed through the analyser will be associated with the orientation of the crystallites, namely their *c* crystallographic axis perpendicular to the fibre axis. Moreover, if the extinctions and the intensity maxima correspond to angles between fibre axis and the polarizer direction of $0 \pm 90°$ and $45 \pm 90°$, respectively, the preferred orientation of the $(0\,0\,2)$ planes will be perpendicular or parallel compared to the fibre axis. Thus, at the light
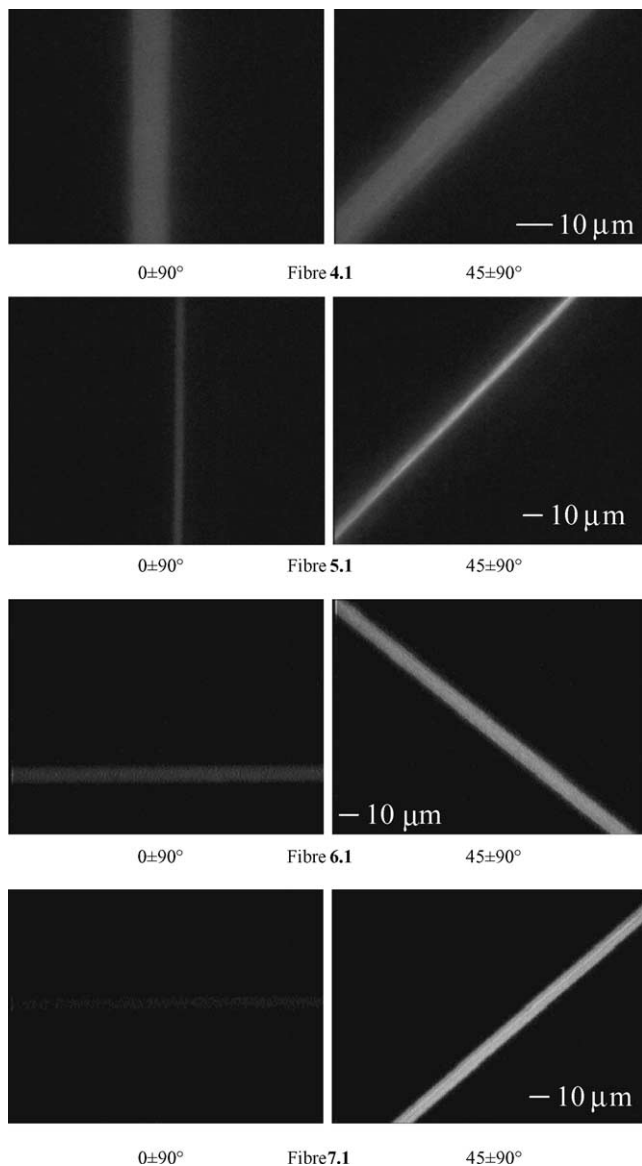
microscopy scale, the orientation of the planes of hexagons $((0\,0\,2)$ planes) with respect to the fibre axis can be directly evaluated by the brightness and the sharpness of the light at $45 \pm 90°$ and conversely by the extinction of the light at $0 \pm 90°$.

Fig. 6 displays images of fibres **4.1**, **5.1**, **6.1** and **7.1** under polarized light. In the four cases, the intensity of the transmitted light is maximal for a position of $45 \pm 90°$. For the position $0 \pm 90°$, the intensity decreases from fibre **4.1** to fibre **7.1**. In the case of fibre **4.1**, this intensity is nearly the same that in position $45 \pm 90°$, while the intensity of the fibre **7.1** in position $0 \pm 90°$ is quite zero. This phenomenon highlights a preferred orientation of the $(0\,0\,2)$ planes, i.e. a texture, at a large scale. One can conclude that these planes are either directed parallel to the axis of fibre (fibre **7.1**) or are randomly oriented around this axis (fibre **4.1**). While basing itself on the XRD results and especially on TEM images associated with SAD patterns, we deduced unambiguously that the layers of hexagons are directed more or less parallel to the fibre axis. The comparison of PLM images of the four fibres shows that the contrast between the two positions (intensity maximum/extinction) as well as the intensity of the reflected light increase following the order **4.1**, **5.1**, **6.1** and **7.1**, which signify that the mean orientation of the basal planes parallel to the axis increases in the same order.

4. Conclusion

The microstructure of fibres **4.1**, **5.1**, **6.1** and **7.1** examined by Transmission Electron Microscopy (TEM) is similar with three concentric parts: epiderm, derma and core with a concomitant increase in crystallites size toward the core of the fibre. However, texture orientation have been revealed with improvements in alignment of crystallites in the order **4.1**, **5.1**, **6.1** and **7.1** fibres. This evolution in the orientation of $(0\,0\,2)$ planes in this series is more obvious with polarized light microscopy because this technique provides interesting informations at a larger scale (several microns). Furthermore, the preferred orientation of crystallites with respect to the fibre axis is associated with an increase in their mechanical properties. On the basis on these examples, we can summerize some relationships between the microstructural and textural states of these boron nitride fibres and their mechanical properties. First of all, boron nitride must display a high crystallinity in its hexagonal form, which requires a high final temperature for the thermal treatment, at least 1600 °C. Then, all the results converge to show that the mechanical properties of the fibres are strongly dependent of the orientation of the layers of hexagons with respect to the fibre axis. However, if we refer to the case of carbon fibres,[9] the Young's modulus *E* is known to be a direct function of the orientation of the graphitic layers whereas strength is ultimately controlled by flaws, even if it depends probably of the alignment of crystallites along the stress direction. In order to clarify this point, systematic studies are necessary in order to determine

Fig. 6. PLM images of fibres **4.1**, **5.1**, **6.1** and **7.1** at angles of $0 \pm 90°$ (extinction) and $45 \pm 90°$ (brightness).

whether the texture could control strenght in the absence of structural flaws.

References

1. Paine, R. T. and Narula, C. K., *Chem. Rev.*, 1990, **90**, 73;
   Paine, R. T. and Sneddon, L. G., *Chemtech*, 1994, **7**, 29.
2. Bernard, S., Ayadi, K., Berthet, M.-P., Chassagneux, F., Cornu, D., Létoffé, J.-M. and Miele, P., *J. Solid State Chem.*, 2004, **177**, 1803.
3. Toury, B., Miele, P., Cornu, D., Vincent, H. and Bouix, J., *Adv. Funct. Mater.*, 2002, **12**, 228.
4. Toury, B., Bernard, S., Cornu, D., Chassagneux, F., Létoffé, J.-M. and Miele, P., *J. Mater. Chem.*, 2003, **13**, 274.
5. JCPDS, data for h-BN are (d/Å) ($h\,k\,l$): 3.33 (0 0 2), 2. 17 (1 0 0), 2.06 (1 0 1), 1. 82 (1 0 2), 1.66 (0 0 4), 1. 25 (1 1 0), 1. 17 (1 1 2).
6. Chassagneux, F., Epicier, T., Toutois, P., Miele, P., Vincent, C. and Vincent, H., *J. Eur. Ceram. Soc.*, 2002, **22**, 2415.
7. Nemanich, R. J., Solin, S. A. and Martin, R. M., *Phys. Rev. B*, 1981, **23**, 6348.
8. Lee, K. J. and Chen, Z. Y., *Mater. Chem. Phys.*, 2003, **82**, 428.
9. Pennock, G. M., Taylor, G. H. and Fitzgerald, J. D., *Carbon*, 1993, **31**, 591.
10. Lee, K. J., Chern Lin, J. H. and Ju, C. P., *Mater. Chem. Phys.*, 2003, **78**, 760.
11. Bortchagovsky, E. G., Reznik, B., Gerthsen, D., Pfrang, A. and Schimmel, T., *Carbon*, 2003, **41**, 2427.